JOURNAL OF MATERIALS SCIENCE **36** (2001) 3641 – 3648

Valence compensated perovskite oxide system $Ca_{1-x}La_xTi_{1-x}Cr_xO_3$

Part I *Structure and dielectric behaviour*

R. K. DWIVEDI
School of Materials Science and Technology, Institute of Technology, Banaras Hindu University, Varanasi 221 005, India

D. KUMAR, O. PARKASH*
Department of Ceramic Engineering, Institute of Technology, Banaras Hindu University, Varanasi 221 005, India
E-mail: oparkash@banaras.ernet.in

Attempts have been made to synthesize compositions with $x = 0.01$, 0.03, 0.05, 0.10, 0.20, 0.30 and 0.50 in the valence compensated system $Ca_{1-x}La_xTi_{1-x}Cr_xO_3$ by solid state ceramic method. Solid solutions form upto $x \leq 0.50$. All the compositions have been found to have orthorhombic structure. The structure of the compositions upto $x \leq 0.10$ is similar to that of $CaTiO_3$. The structure changes gradually from $CaTiO_3$ to $LaCrO_3$ in the composition range $0.10 < x < 0.50$. Dielectric constant, at room temperature, has been found to increase with increasing substituent concentration upto $x = 0.30$ and thereafter it decreases with increasing x upto 0.50. Orientational and space charge polarizations contribute to the dielectric behaviour of these materials.

1. Introduction

Calcium titanate, $CaTiO_3$ is a perovskite oxide having orthorhombic symmetry [1]. It is paraelectric at room temperature, having dielectric constant ~180 and dielectric loss $\sim 10^{-3}$ at 1 kHz. Extensive research has been carried out on this oxide to improve its dielectric properties. Yttrium doped calcium titanate, when heated in an atmosphere of low partial pressure of oxygen, becomes semiconducting and exhibits relaxor behavior characteristic of barrier layers [2]. On replacing divalent calcium by trivalent yttrium or other rare earth ions, the charge neutrality is maintained by creating an appropriate number of vacancies on calcium sites [2, 3]. On the otherhand, Lewis and Catlow [4] have reported that donor substitution on A-site will lead to the formation of titanium vacancies to maintain electrical charge neutrality. The acceptor dopants such as K^+ and Fe^{3+} will generate oxygen vacancies [5]. During the last few years, some investigations on the electrical properties of alkaline earth titanates doped simultaneously with La^{3+} or Y^{3+} on alkaline earth ion sites and Co^{3+}, Ni^{3+} on titanium sites have been made. These materials are found to exhibit interesting and useful electrical properties [6, 7]. For example compositions with $0.20 \leq x \leq 0.40$ in the system $Sr_{1-x}La_xTi_{1-x}Co_xO_3$ exhibit relaxor like behaviour [8]. These compositions have high value of dielectric constant. This has been explained in terms of barrier layer formation at the grain boundaries.

In this paper we are reporting the results of our investigations on an analogous system $Ca_{1-x}La_xTi_{1-x}Cr_xO_3$ which represents a valence compensated solid solution between $CaTiO_3$ and $LaCrO_3$ where calcium is expected to be replaced by lanthanum and titanium is expected to be replaced by chromium. We have restricted our studies to $x \leq 0.50$ because of our interest in the dielectric properties. Lanthanum chromite has an orthorhombic structure with space group Pbnm. Sr doped $LaCrO_3$ has potential applications as high temperature electrode materials in fuel cells because of its high electrical conductivity and thermal stability [9]. In part II we shall be reporting the electron transport properties of these materials using the results of DC and AC conductivity and Seebeck coefficient measurements.

2. Experimental

Calcium carbonate, lanthanum oxalate, titanium dioxide and chromium oxide, all of Analytical Reagent grade having purity >99.5%, were used as starting materials. Stoichiometric amounts of various chemicals were accurately weighed and mixed in a ball mill for six hours using acetone as a mixing medium. The mixed powders were dried and calcined in a platinum crucible at 1250°C for 12 hours. The calcined powders were ground and mixed with appropriate quantities of 2% solution of polyvinyl alcohol as binder followed

* Author to whom all correspondence should be addressed.

by pressing as cylindrical pellets having thickness in the range 1–2 mm and diameter 1.0 to 1.2 cm using a hydraulic press.

These pellets were slowly heated upto 600°C and kept at this temperature for about an hour to burn off the binder completely. Thereafter, the temperature was raised to 1400°C at which both sintering as well as solid state reaction amongst various constituents take place. These pellets were maintained at their respective firing temperatures for eight hours. After firing, the furnace was cooled at the rate of 5–6°C per minute upto 600°C and then it was switched off. The sintered pellets were powdered and examined using X-ray diffraction to confirm the formation of single phase materials. X-ray diffraction patterns were recorded using Rigaku Rotaflex RTP 300, X-ray Diffractometer employing Cu-$K_{\alpha 1}$ radiation. XRD data were indexed. Density of the sintered pellets was determined from the geometrical dimensions and their mass as well as Archemede's principle. Theoretical density or the X-ray density was determined from the lattice parameters and molecular weight of the samples.

For microstructural studies, pellets were polished using emery papers (1/0, 2/0, 3/0 and 4/0), followed by polishing on a silk cloth with diamond paste of the grade 3 μm, 1 μm and 1/4 μm. The pellets were cleaned using distilled water followed by methanol. Then these were thermally etched by keeping at 1400°C for 20 minutes. These were then coated with Au-Pd alloy by sputtering and the micrographs were recorded using, Jeol SEM 800 scanning electron microscope (SEM). Two pellets in each composition were coated with Ag-Pd paint and fired at 800°C for half an hour to cure the paint. Capacitance and dissipation factor were measured at different frequencies employing HP 4192 A impedance analyzer at different steady temperatures in the temperature range 100–550 K. Measurements were made during heating and cooling to check the reproducibility of the results on two pellets of each sample.

3. Results

3.1. Crystal structure, density and microstructure

Powder X-ray diffraction of all the prepared compositions showed the formation of single-phase solid solutions. The formation of single phase was confirmed by the absence of the characteristic x-ray diffraction lines of the constituent oxides and other phases in the x-ray diffraction (XRD) patterns. Powder x-ray diffraction (XRD) data of the compositions with $x \leq 0.10$ could be indexed on the basis of an orthorhombic unit cell with space group Pcmn similar to $CaTiO_3$. For compositions with $x > 0.10$, the structure changes from orthorhombic symmetry with space group Pcmn of $CaTiO_3$ to another orthorhombic symmetry with space group Pbnm of $LaCrO_3$. XRD data of the compositions within the range $0.20 < x \leq 0.50$ have been indexed on the basis of unit cell of $LaCrO_3$ structure.

The lattice constants for all the compositions were calculated using the program 'CEL'. The difference between the ionic radii of Ca^{2+} (1.35 Å) and La^{3+} (1.32 Å) or between the ionic radii of Ti^{4+} (0.605 Å) and Cr^{3+} (0.615 Å) is very small. This explains almost constant unit cell volume of the compositions with $x \leq 0.10$. The slight increase in the unit cell volume for $x \geq 0.20$, may be due to change in the crystal structure. Lattice parameters, structure, unit cell volume and % porosity of all the samples are given in Table I.

The scanning electron micrographs of the various samples are shown in Fig. 1. The average grain size in each of these samples was measured by line intercept method and is given in Table I. Average grain size has been found to increase with increasing x upto $x = 0.10$. As long as the structure follows orthorhombic symmetry of $CaTiO_3$, grain growth has been observed. When the structure changes from symmetry of $CaTiO_3$ to that of $LaCrO_3$ with increasing x, the grain growth has been found to be inhibited. The exact reason for this behaviour is not known at present. In the composition range $0.20 < x \leq 0.50$, the grain size has been found to be small. $LaCrO_3$ requires high temperature for sintering due to its refractory nature [10]. Refractoriness increases with increasing x in the present system. We could not sinter the present samples at such a high temperature (1700°C) due to our experimental limitations. Small grain size for samples with $x > 0.20$, may be due to low sintering temperature used in their preparation.

3.2. Dielectric behaviour

Typical plots of dielectric constant, ε_r and dissipation factor D vs temperature at 1, 10 and 100 kHz for $x = 0.10$ and 0.30 are shown in Figs 2-3a and Figs 2-3b

TABLE I Structure, lattice parameters, unit cell volume, percentage porosity and average grain size for various compositions (x) in the system $Ca_{1-x}La_xTi_{1-x}Cr_xO_3$

Composition (x)	Lattice parameters			Structure	Unit cell volume (m^3)	Percentage porosity	Grain size (μm)
	a (Å)	b (Å)	c (Å)				
0.00	5.445 ± 0.002	7.644 ± 0.005	5.384 ± 0.004	Orthorhombic	224.09×10^{-30}	2	
0.01	5.445 ± 0.003	7.645 ± 0.003	5.386 ± 0.002	Orthorhombic	224.20×10^{-30}	6	1
0.03	5.445 ± 0.005	7.647 ± 0.003	5.382 ± 0.004	Orthorhombic	224.09×10^{-30}	4	3
0.05	5.446 ± 0.005	7.650 ± 0.006	5.371 ± 0.005	Orthorhombic	223.73×10^{-30}	9	6
0.10	5.442 ± 0.002	7.644 ± 0.003	5.427 ± 0.002	Orthorhombic	225.83×10^{-30}	10	12
0.20	5.483 ± 0.029	5.438 ± 0.029	7.670 ± 0.040	Orthorhombic	228.68×10^{-30}	10	2
0.30	5.489 ± 0.047	5.464 ± 0.047	7.669 ± 0.066	Orthorhombic	230.03×10^{-30}	11	2
0.50	5.578 ± 0.009	5.455 ± 0.009	7.739 ± 0.013	Orthorhombic	236.49×10^{-30}	12	1

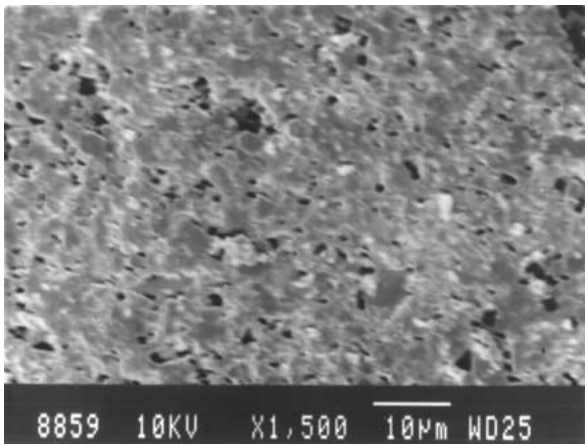

(a)

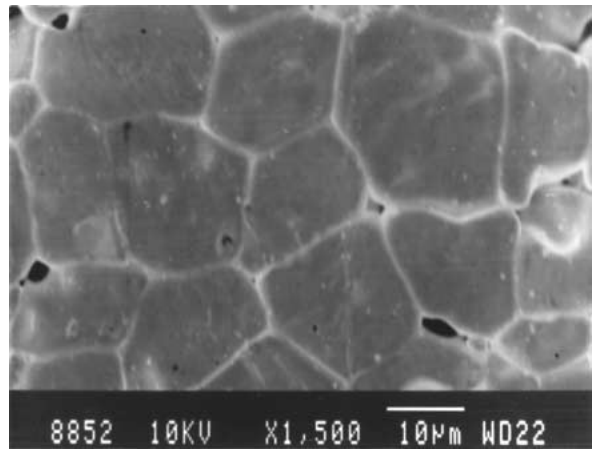

(d)

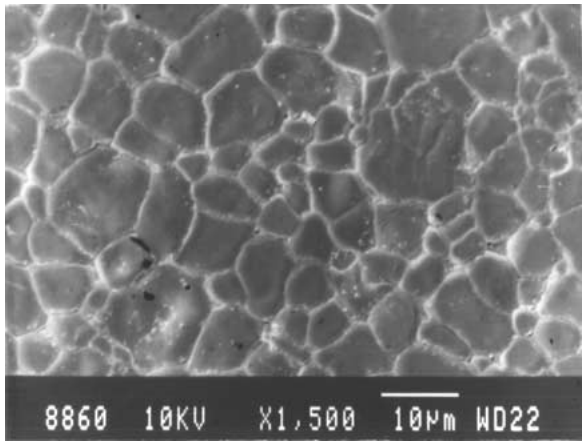

(b)

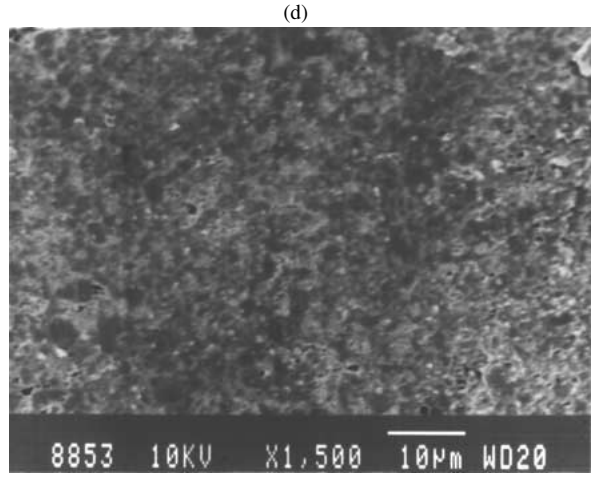

(e)

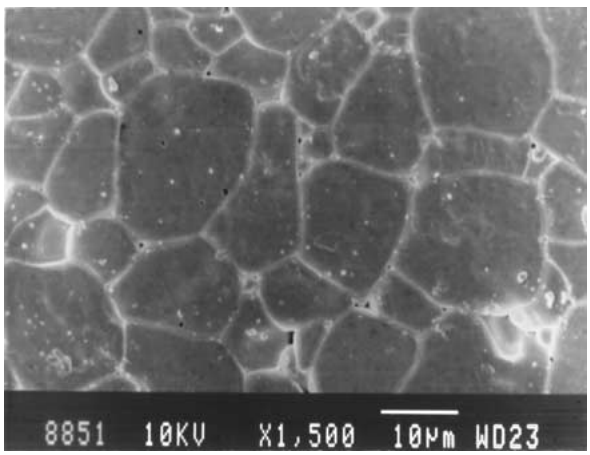

(c)

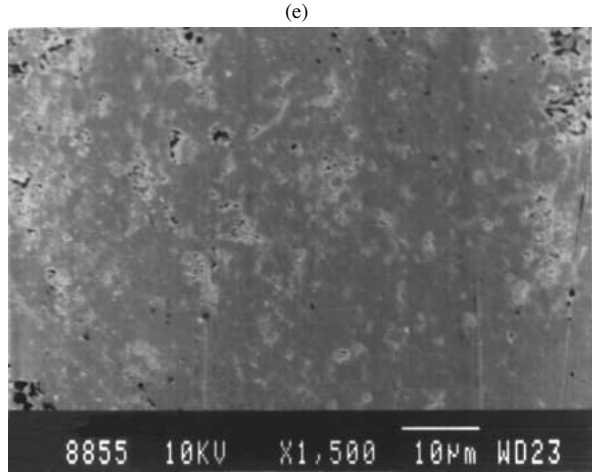

(f)

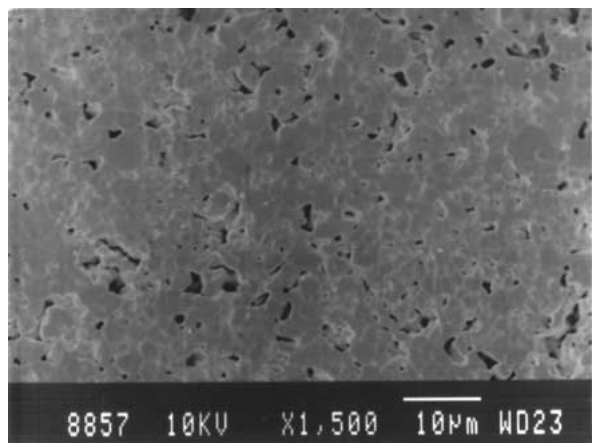

(g)

Figure 1 Scanning electron micrographs of thermally etched surfaces of samples with x (a) 0.01, (b) 0.03, (c) 0.05, (d) 0.10, (e) 0.20, (f) 0.30 and (g) 0.50 in the system $Ca_{1-x}La_xTi_{1-x}Cr_xO_3$.

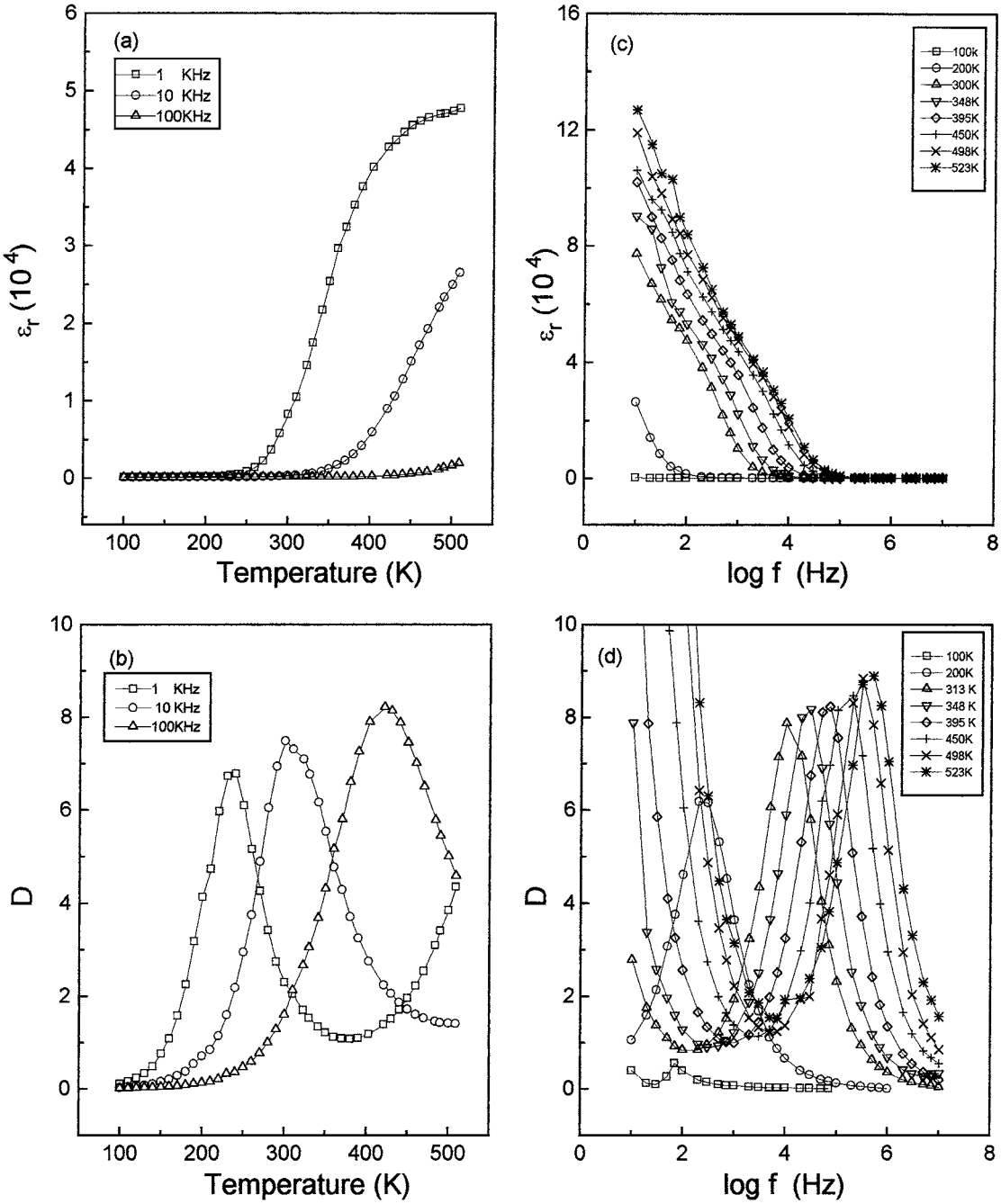

Figure 2 Variation of (a) ε_r and (b) D with temperature at 1, 10 and 100 kHz; (c) ε_r and (d) D with log frequency at a few steady temperatures for the composition $Ca_{0.90}La_{0.10}Ti_{0.90}Cr_{0.10}O_3$.

respectively. ε_r vs log f and D vs log f plots for these compositions at a few steady temperatures are given in Figs 2-3c and Figs 2-3d respectively. It is noted that ε_r for all the compositions initially remains constant with temperature upto a particular temperature T_a beyond which it increases rapidly with temperature. T_a decreases with increasing x for a particular frequency and increases with frequency for the same composition. For $x = 0.10$, ε_r vs T plot levels off (an anomaly) at high temperature at 1 kHz after a rapid rise with temperature. At other frequencies, for this composition, leveling off seems to occur beyond our temperature range of measurement. For $x = 0.20$, 0.30 and 0.50 there is a very rapid rise in ε_r after the second plateau in ε_r vs T plots. The second plateau in ε_r vs T plots occurs in the intermediate temperature range which is followed by a steep rise in dielectric constant at high temperature.

D vs T plots exhibit a peak (Figs 2b and 3b). Similar behaviour is observed in other compositions also. The temperature of the peak increases with with increasing frequency. It decreases at a particular frequency with increasing x. Frequency dependence of ε_r (Figs 2c and 3c) shows that ε_r remains independent of frequency at low temperature (100 K). At higher temperatures, a frequency dependent region is observed in the low frequency range and it becomes independent of frequency in the higher frequency range. There is a rapid rise of ε_r at low frequencies. The frequency, below which a rapid rise sets in, increases with increasing temperature. For compositions with $x = 0.05$ and 0.10, a Debye type relaxation is observed in ε_r vs log f plots. For

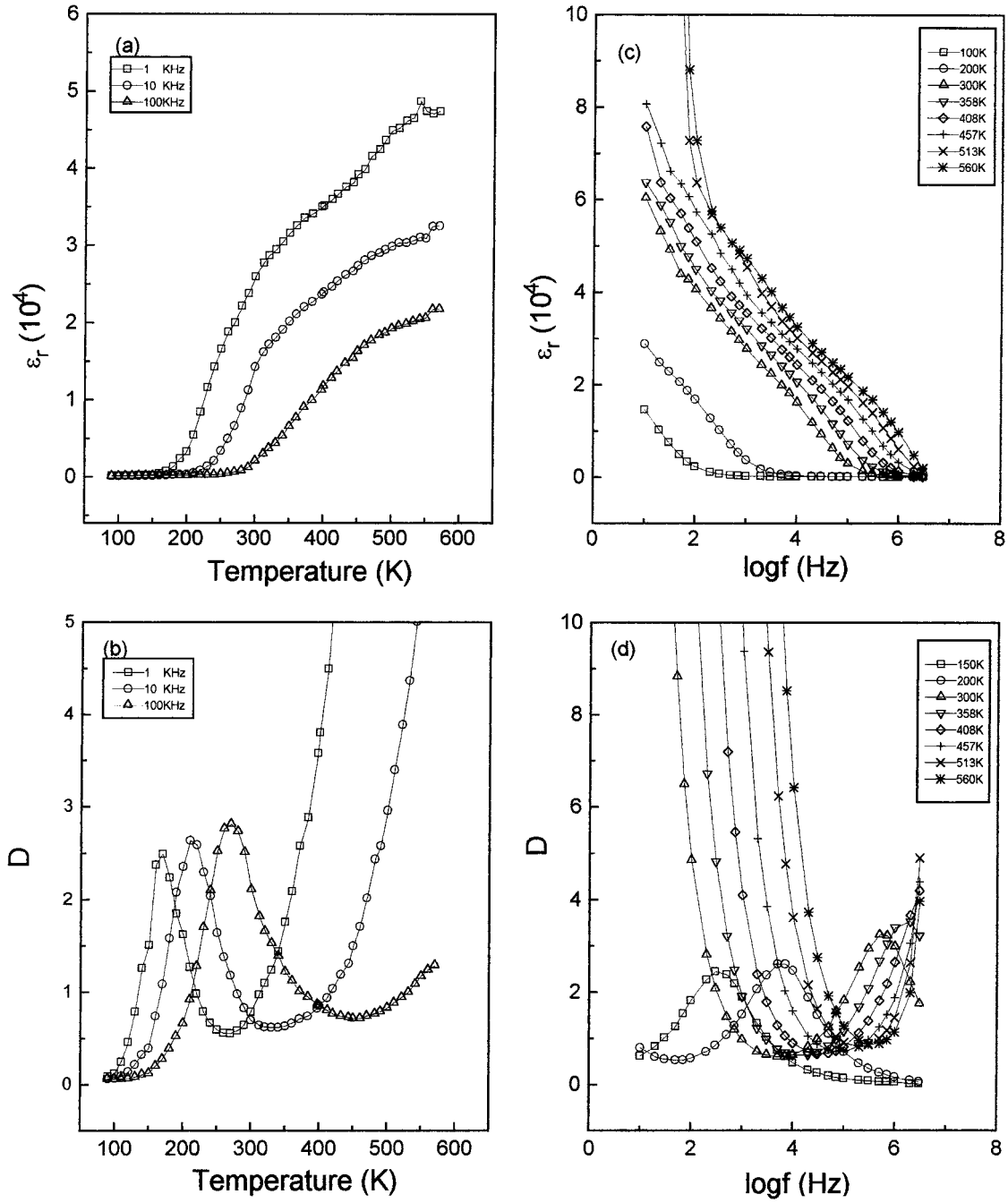

Figure 3 Variation of (a) ε_r and (b) D with temperature at 1, 10 and 100 kHz; (c) ε_r and (d) D with log frequency at a few steady temperatures for the composition $Ca_{0.70}La_{0.30}Ti_{0.70}Cr_{0.30}O_3$.

$x = 0.20, 0.30$ and 0.50, two Debye type relaxations are clearly observed within the frequency range of measurements. The relaxation frequencies for both the processes move to higher frequency side with increasing temperature.

D vs log f plots (Figs 2d and 3d) show a peak. This peak corresponds to the high frequency relaxation observed in ε_r vs log f plots. D increases very rapidly at low frequencies at high temperature. The frequency, at which D starts increasing rapidly, increases with increasing temperature. A peak appears in D vs log f plot where the relation $\omega\tau = 1$ is satisfied where ω, the angular frequency $= 2\pi f$, f being the frequency in cycles per second and τ is the relaxation time for a particular polarization process. Values of τ were determined from the peak frequencies at different temperatures. Plots of log τ vs 1000/T are shown in Fig. 4. for various compositions. These plots are linear showing that τ obeys the Arrhenius relationship

$$\tau = \tau_0 \exp \frac{E_{rel}}{kT} \tag{1}$$

where E_{rel} is the activation energy for the relaxation process. The values of E_{rel} are determined by least square fitting of the data and are given in Table II. E_{rel} is higher in high temperature range and lower in low temperature range. Compositions with $x = 0.05$ and 0.10 have equal values of E_{rel}. Similarly $x = 0.20$ and 0.30 have equal values of E_{rel}. E_{rel} for $x = 0.20$ and 0.30 is slightly less than that of $x = 0.05$ and 0.10. E_{rel} could not be obtained for $x = 0.50$ due to lack of sufficient data in the temperature range of measurement.

TABLE II Values of activation energy, E_{rel} and relaxation times, τ_o for various compositions (x) in the system $Ca_{1-x}La_xTi_{1-x}Cr_xO_3$

Composition (x)	E_{rel} (eV)		Relaxation time (τ_o) (s)	
	200 K–350 K	350 K–550 K	200 K–350 K	350 K–550 K
0.03	0.13	0.27	2.26×10^{-6}	4.66×10^{-9}
0.05	0.14	0.26	4.49×10^{-7}	2.78×10^{-9}
0.10	0.13	0.26	1.27×10^{-7}	9.37×10^{-10}
0.20	0.12	0.21	1.20×10^{-8}	1.72×10^{-10}
0.30	—	0.21	—	1.21×10^{-10}
0.50	—	—	—	—

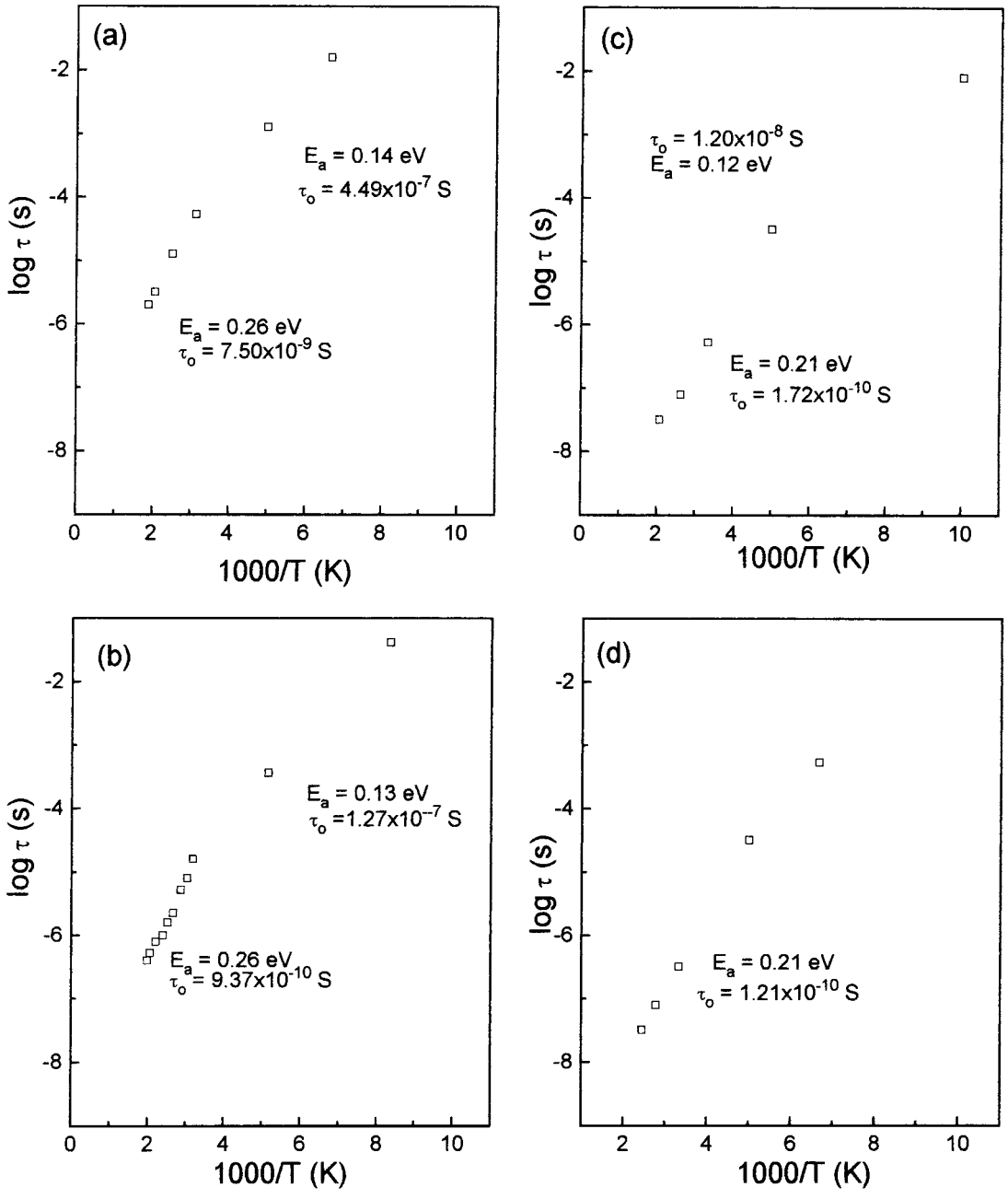

Figure 4 Plots of log τ vs 1000/T for compositions x (a) 0.05, (b) 0.10, (c) 0.20 and (d) 0.30 in the system $Ca_{1-x}La_xTi_{1-x}Cr_xO_3$.

4. Discussion

Debye type peaks are observed in D vs T or D vs log f plots of all the compositions. These peaks are observed only at certain temperatures in the frequency range of measurements. This may be due to the orientational polarization present in the bulk. These materials are sintered at high temperatures where they are expected to lose traces of oxygen according to the reaction:

$$O_O \leftrightarrow 1/2O_2 + V_O^{\bullet\bullet} + 2e' \qquad (2)$$

where all the species are written in accordance with Kröger–Vink notation of defects. Oxygen vacancies exist in doubly ionized state above 550°C. Below this

temperature they change to singly ionized state $V_O^{\bullet}$ [11–13] as per the reaction

$$V_O^{\bullet\bullet} + e' \leftrightarrow V_O^{\bullet} \quad (3)$$

These oxygen vacancies act as intrinsic donors. Some of the oxygen vacancies are in the doubly ionized state at room temperature. This is due to freezing of high temperature state of oxygen vacancies ($V_O^{\bullet\bullet}$) because of rapidly falling temperature after sintering. Trivalent La^{3+} ions, substituted on Ca^{2+} sites act as a extrinsic donors. Similarly trivalent Cr^{3+} ions on Ti^{4+} site act as extrinsic acceptors. Cr^{3+} ion on Ti^{4+} sites carries an effective unit negative charge i.e. $Cr_{Ti^{4+}}^{3+\prime}$. These $V_O^{\bullet}$ and $V_O^{\bullet\bullet}$ and $Cr_{Ti^{4+}}^{3+\prime}$ may form dipoles of the type $(Cr_{Ti^{4+}}^{3+\prime} - V_0^{\bullet})$ or $(2Cr_{Ti^{4+}}^{3+\prime} - V_0^{\bullet\bullet})$ due to coulombic attraction. These dipoles can change orientation due to hopping of holes among Cr_{Ti}^{x} and $Cr_{Ti}^{\prime}$ sites. Another process, which may occur is the hopping of holes among $V_0^{\bullet}$ and $V_0^{\bullet\bullet}$ which will again lead to change in orientation of dipoles. The values of activation energies calculated from the Arrhenius plots of relaxation times vs inverse of temperature are given in the Table II. At low temperatures, (200–350 K) these are around 0.10 eV and at high temperature (350–550 K) these are around 0.25 eV. The values of activation energies obtained from log τ vs 1000/T plots agree with the values obtained from the log σ_{ac} vs 1000/T plots. Values of σ_{ac} were obtained from the plateaus observed in log σ_{ac} vs log f plots (to be discussed in part II). This shows that both polarization and conduction occurs due to the same mechanism.

These materials exhibit low values of DC conductivity at low temperatures. This may be due to trapping of charge carriers (hopping sites) in the associated defect pairs as mentioned above. With increasing temperature, these charge carriers get released due to dissociation of these defect pairs. Therefore, with increasing temperature, DC conductivity increases due to long range movement of these charge carriers through the bulk. But these charge carriers get intercepted at the grain–grain boundaries which act as barriers for their cross transport [11, 12]. This gives rise to space charge polarization at grain–grain boundaries interfaces. The space charge polarization increases with increasing temperature due to exponential increase of conductivity with temperature. This is manifested by a rapid rise in dielectric constant with temperature in the high temperature range. This contribution of space charge polarization is clearly seen in ε_r vs log f plots of compositions with $x = 0.20$ and 0.30 in the lowest frequency region. The capacitance associated with this contribution is in the nano-farad range. This order of capacitance is assigned to thin regions like grain boundaries. This contribution appears only above a certain temperature. This is because at lower temperatures, the dc conductivity due to long range movement of the charge carriers is small. It increases exponentially with temperatures.

Nowick *et al.* [14] observed dielectric relaxation peaks at low temperatures in acceptor doped potassium tantalate and calcium titanate. They determined the activation energies for this relaxation process and found these in the range 0.10–0.40 eV. They ascribed this relaxation to orientational polarization arising due to formation of associated defects of the type $M_{Ta}'' - V_O^{\bullet\bullet}$ $M_{Ti}'' - V_O^{\bullet\bullet}$ where M represents trivalent or divalent acceptor on Ta or Ti sites. The change in orientation of dipoles occurs due to jumping of $V_0^{\bullet\bullet}$ in $TiO_5 - V_0^{\bullet\bullet}$ octahedra. They explained low values of activation energies due to sufficient readjustment of ions around the impurity atoms (acceptor dopants) which ease the jumping of oxygen ions with low value of activation energy. This mechanism, however, does not contribute to the DC conduction. But we have observed in our samples that conduction and dielectric relaxation occurs due to the same process as mentioned above. The dielectric relaxation, therefore, seems to be Debye type due to hopping of electronic charge carriers.

The values of τ obtained by us in the low temperature (200–300 K) region are of order of 10^{-5} second. These values are higher than that obtained from Mössbauer studies of the $Eu_{1-x}Sr_xFeO_3$ ($x \leq 0.50$) [15] system which were of the order of $\sim 10^{-6}$ seconds at 77 K. Conduction occurs in these materials by hopping of holes among Fe^{3+} and Fe^{4+} ions. These materials exhibited Mössbauer spectra characteristic of Fe^{3+} and Fe^{4+} states upto 400 K, above which they exhibited Mössbauer spectra of time averaged electronic configuration 3.5. This indicated that hopping times were more than 10^{-7} second below 400 K and less than this above 400 K. The higher values of τ in the present materials may be due to higher disorder and larger separation between the hopping sites as compared to the above mentioned system.

5. Conclusion

Solid solution forms in all the compositions investigated i.e. for $x \leq 0.50$. Crystal structure of the compositions with $x \leq 0.10$ is similar to $CaTiO_3$ while compositions with $x \geq 0.20$ have structure similar to $LaCrO_3$. Average grain size is small due to low sintering temperature of these samples. Sinter-ability decreases with increasing x. Dielectric behaviour reveals the presence of orientational and space charge polarization processes.

Acknowledgements

Financial support from Department of Science and Technology, Government of India is gratefully acknowledged. We are thankful to Prof. D. Pandey, Coordinator, School of Materials Science and Technology and Head, Department of Metallurgical Engineering, Institute of Technology, Banaras Hindu University for providing x-ray diffraction and scanning electron microscopic facilities respectively.

References

1. H. F. KAY and P. C. BAILEY, *Acta. Cryst* **10** (1957) 219.
2. S. NEIRMAN and I. BURN, *J. Mater. Sci.* **19** (1984) 737.
3. U. BALACHANDRAN and N. G. EROR, *ibid.* **23** (1988) 2676.
4. G. V. LEWIS and C. R. A. CATLOW, *J. Phys. Chem. Solids* **47** (1986) 89.
5. B. JAFFE, J. W. R. COOK and H. JAFFE, "Piezoelectric Ceramics" (Academic Press, New York, 1971), Chap. 5.

6. CH. D. PRASAD, Ph.D. Thesis, Banaras Hindu University, Varanasi, India, 1988.
7. H. S. TEWARI, Ph.D. Thesis, Banaras Hindu University, Varanasi, India, 1994.
8. OM PARKASH, CH. D. PRASAD and D. KUMAR, *J. Mater. Sci.* **25** (1990) 487.
9. D. B. MEADOWCROFT, *Brit. J. App. Phys.* **2** (1969) 1225.
10. L. GROUPP and H. U. ANDERSON, *J. Amer. Ceram. Soc.* **59** (1976) 449.
11. R. MOOS, Ph.D. Thesis, University of Karlsruhe, Germany, 1994.
12. R. MOOS and K. H. HARDTL, *J. Amer. Ceram Soc.* **80** (1997) 2549.
13. C. LEE, J. DESTRY and L. J. BREBNERC, *Phy. Rev.* **B11** (1975) 2299.
14. A. S. NOWICK, S. Q. FU, W. K. LEE, B. S. LIM and J. SCHERBAN, *Mater. Sci. Engg.* **B23** (1994) 19.
15. VEENA JOSHI, OM PARKASH, G. N. RAO and C. N. R. RAO, *Faraday Transaction II* **75** (1979) 1199.

Received 11 February 2000
and accepted 6 February 2001